American Mineralogist, Volume 77, pages 19–29, 1992

X-ray powder diffraction and ^{23}Na, ^{27}Al, and ^{29}Si MAS-NMR investigation of nepheline-kalsilite crystalline solutions

GUY L. HOVIS*
Department of Geology, Lafayette College, Easton, Pennsylvania 18042, U.S.A.
DANE R. SPEARING, JONATHAN F. STEBBINS
Department of Geology, Stanford University, Stanford, California 94305, U.S.A.
JACQUES ROUX
CNRS-CRSCM, 1A rue de la Ferollerie, 45071 Orleans Cedex-2, France
APRIL CLARE
Department of Geological Sciences, Rutgers University, New Brunswick, New Jersey 08903, U.S.A.

ABSTRACT

Specimens of both natural (Monte Somma) and synthetic Na-rich nepheline have been used to synthesize two ion-exchange series, ranging in composition to pure kalsilite. Excess Si in the natural and synthetic series was 5.2 and 1.7 mol%, respectively. The associated vacancies (VAC) in the alkali sites were found to play an important role in the crystal chemical behavior of these minerals. Room temperature X-ray powder diffraction measurements revealed the presence of three phases in each series: nepheline from sodic compositions to 0.64 (± 0.01) mole fraction K + VAC, tetrakalsilite at 0.72 (± 0.02) K + VAC, and kalsilite above 0.80 K + VAC, with a narrow miscibility gap between K-rich nepheline and tetrakalsilite. Increases of *a, c,* and volume were linear with K content within each structural region. However, for nepheline the increases accelerated beyond compositions at which K (or K + VAC) was forced to occupy Na structural positions. For the more vacancy-rich natural series this occurred at lower K contents, suggesting preference of vacancies for the larger alkali position. The overall effect of □Si exchange in nepheline, in fact, was found to resemble that of large-ion substitution in the alkali site. Both the nepheline to tetrakalsilite and tetrakalsilite to kalsilite transitions were accompanied by apparent discontinuities in the *c* unit-cell dimension. Unit-cell volume was discontinuous for a hypothetical nepheline to kalsilite transition. Magic-angle-spinning (MAS) NMR data of ^{23}Na, ^{27}Al, and ^{29}Si for part of the natural series suggest that the nepheline structure is distorted on both a local (unit-cell) and long-range scale with the addition of K. Similarly, the kalsilite structure is distorted with increasing Na content. Stoichiometric nepheline (K + VAC = 0.25) is observed to have the least distorted tetrahedral sites as calculated from the ^{27}Al quadrupolar coupling constant. Lastly, the ^{29}Si and ^{27}Al NMR suggest complete ordering between the Si and Al tetrahedral sites, thus preserving the Al avoidance rule.

INTRODUCTION

Nepheline-kalsilite solid solutions constitute an important group of rock-forming silicates. Even so, little is known quantitatively about the thermodynamic mixing properties of these minerals. As a first step in determining these properties, Hovis and Roux (in preparation) synthesized two nepheline-kalsilite ion-exchange series. They reported on acid-solution calorimetric measurements made to determine enthalpies of K-Na mixing in the two series. It is the purpose of the present paper to report on the unit-cell dimensions and volumes across the series and on investigation of the series using nuclear magnetic resonance (NMR) spectroscopy.

Although the nepheline-kalsilite series is commonly thought to involve only K-Na substitution, these solid solutions may also vary in Al:Si ratio and in the degree to which various elements substitute for K and Na. Thus, vacancies created by the coupled □Si = (K,Na)Al substitution, as well as by chemical variation such as □Ca = 2(K,Na), become an additional compositional variable in the system. The details of the structures of nepheline group minerals, all stuffed derivatives of high tridymite, have been summarized well by Merlino (1983; also see Hovis and Roux, in preparation). Phases encountered during the

* Present address: Division of Earth Sciences, National Science Foundation, Washington, DC 20550, U.S.A.

0003–004X/92/0102–0019$02.00

TABLE 1. Chemical compositions of nepheline-kalsilite crystalline solutions

Sample	Ne	Ks	0.5An	2Qz*
		Natural series		
8311	0.747	0.129	0.072	0.052
8861	0.710	0.171	0.067	0.052
8718	0.671	0.215	0.061	0.052
8811	0.618	0.273	0.057	0.052
8862	0.560	0.335	0.053	0.052
8808	0.500	0.400	0.048	0.052
8925	0.441	0.465	0.042	0.052
8929	0.357	0.557	0.034	0.052
8937	0.346	0.569	0.033	0.052
8928	0.252	0.672	0.025	0.052
8807	0.193	0.736	0.019	0.052
8723	0.132	0.802	0.015	0.052
8719	0.008	0.937	0.003	0.052
8860	0.000	0.948	0.000	0.052
		Synthetic series		
880408	0.933	0.050	NA	0.017
8824	0.875	0.108	NA	0.017
8825	0.821	0.162	NA	0.017
8826	0.765	0.218	NA	0.017
8827	0.668	0.315	NA	0.017
8834	0.574	0.409	NA	0.017
8853	0.484	0.499	NA	0.017
8847	0.422	0.561	NA	0.017
8908	0.354	0.629	NA	0.017
8843	0.285	0.698	NA	0.017
8828	0.193	0.790	NA	0.017
8829	0.097	0.886	NA	0.017
8823	0.000	0.983	NA	0.017

Note: Compositions given as mole fractions of Ne = $NaAlSiO_4$, Ks = $KAlSiO_4$, 0.5An = $\square_{0.5}Ca_{0.5}AlSiO_4$, 2Qz = $\square SiSiO_4$, where $\square$ = vacancies. NA = not analyzed for Ca.

* The 2Qz contents of 0.052 and 0.017 for members of the natural and synthetic series are based on data for members on which full chemical analyses for K, Na, Ca, Al, and Si were performed. Otherwise compositions for these members are based on partial analyses for K, Na, and Ca only or on the weights and compositions of the parent materials used to make the specimens (see Hovis and Roux, in preparation).

present study—nepheline, tetrakalsilite, and kalsilite—are all refined in space group $P6_3$, yet each is unique in the type(s) and proportion of six-membered tetrahedral rings (hexagonal, oval, and ditrigonal). This in turn affects the type(s) and proportions of alkali sites in each structure. For example, nepheline has two types of alkali sites, correlating with its hexagonal and oval rings, the smaller Na sites outnumbering the larger K sites by 3:1. Kalsilite has only ditrigonal rings. Tetrakalsilite has all three kinds of rings based on structural analysis of its natural analogue, panunzite (Benedetti et al., 1977).

Chemical data for all materials studied in this investigation are given by Hovis and Roux (in preparation). For convenience, however, compositions are summarized in Table 1 using the components nepheline (Ne = $NaAlSiO_4$), kalsilite (Ks = $KAlSiO_4$), "half anorthite" (0.5An = $\square_{0.5}Ca_{0.5}AlSiO_4$), and "twice quartz" (2Qz = $\square SiSiO_4$). Mole fractions of vacancies (hereafter denoted as VAC) can be calculated by summing half the 0.5An and all of the 2Qz component for each sample.

STARTING MATERIALS AND SYNTHESIS PROCEDURES

The ion-exchange series made for this study were based on specimen 8311, natural nepheline from Monte Somma obtained from Enrico Franco (Naples University), containing 5.2 mol% excess Si (i.e., 2Qz = 0.052, molar Al:Si = 0.948:1.052) and 0.036 Ca ions per four O atoms, and on specimen 880408, made synthetically by crystallizing a mechanical mixture of two end-member gels at 800 °C and 2 kbar over a 72-h period. Gels for the synthetic parent were prepared using the method of Hamilton and Henderson (1968), and crystallization was conducted in an internally heated pressure vessel fitted with a high-performance furnace. A molar K content of 0.050 was produced in order to avoid highly twinned material typical of the pure Na end-member (Henderson and Roux, 1977). The well-crystallized product, which included many coarse euhedral grains, was found by atomic absorption and electron microprobe techniques to have 1.7% excess Si (2Qz = 0.017, molar Al:Si = 0.983:1.017), accounting for its total of 0.017 VAC.

The parent material of each ion-exchange series was used to make a corresponding kalsilite end-member by ion-exchange in molten KCl. Intermediate compositions were made by combining the kalsilite samples with the respective parent materials in various proportions to produce the desired bulk compositions. These powders were mixed well in acetone, dried, and compressed into Pt crucibles. They were then annealed at high temperatures, with periodic remixing, in order to homogenize the K and Na ions. Details of the synthesis histories of individual series members are given by Hovis and Roux (in preparation).

Members of the ion-exchange series made from parent materials 8311 and 880408 shall henceforth be referred to as belonging either to the natural or synthetic series, respectively. In the natural series, Ca and VAC vary with Na/K ratio, in both cases decreasing toward the K end of the series as a result of the coupled $\square Ca = 2K$ exchange. VAC thus reaches the minimum of 0.052 in the pure kalsilite end-member, equal to the mole fraction of 2Qz for the series. The synthetic series on the other hand is strictly an Na-K exchange series with a constant VAC of 0.017 for all members.

X-RAY POWDER DIFFRACTION RESULTS

X-ray techniques

X-ray scans were made over a 12–70° 2θ range at 0.25°/min with a Scintag Pad V automated diffractometer utilizing filtered Cu radiation, slits of 0.3 and 0.5 mm, and a monochromatized detection system. Diffraction maxima were located with Scintag's Peakfinder program. Cu$K\alpha_2$ peaks were mathematically stripped. Unit-cell dimensions were calculated by entering the $K\alpha_1$ data, hand corrected based on an internal Si standard (NBS reference material 640a having a stated unit-cell dimension of 5.430825 Å) into Burnham's (1962) LCLSQ lattice constant refinement program assuming a Cu$K\alpha_1$ wavelength of 1.54051 Å. X-ray diffraction maxima were indexed using JCPDS file data for nepheline (35-424, Keller and McCarthy, 1984; 9-338, Smith and Tuttle, 1957), kalsi-

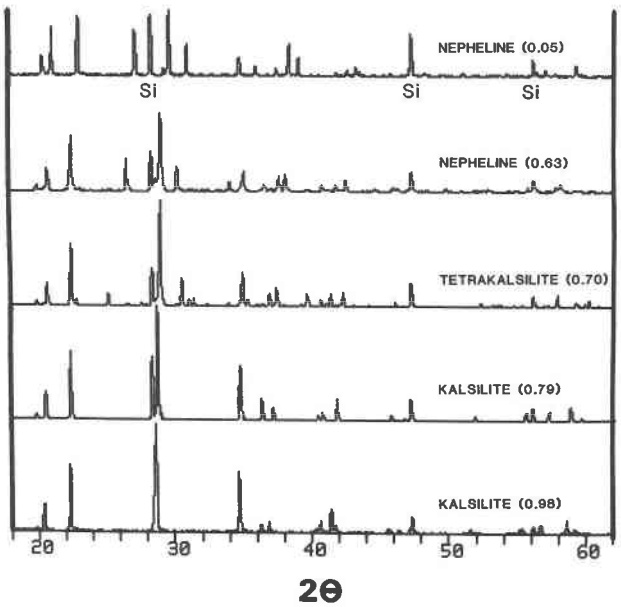

Fig. 1. X-ray powder diffraction data for five members of the synthetic nepheline-kalsilite series. Mole fraction Ks is in parentheses after each mineral name and can be correlated with individual specimens using Table 1. Note that peaks at 28.4°, 47.3°, and 56.1° (labeled in top diffractogram) are from the Si internal standard and are common to all patterns. Values of 2θ are for Cu$K\alpha_1$ radiation.

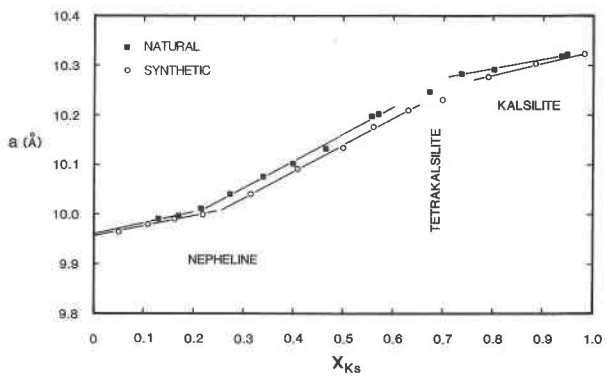

Fig. 2. Variation of the a unit-cell dimension with X_{Ks} (= mole fraction kalsilite). Data for all phases are normalized to the 10 Å unit cell of nepheline. Upper and lower sets of lines are least-squares regressions to the natural and synthetic series data, respectively, within each structural region. Because of the presence of vacancies, the most potassic data point for each series is its end point; thus, lines are not extended to the $X_{Ks} = 1$ border. Note the kink in a in the nepheline structural region; this occurs at more potassic compositions in the synthetic series than in the natural series, as discussed in the text. Equations for the lines are given in Table 4.

lite (11-579, Smith and Tuttle, 1957), and tetrakalsilite-panunzite (11-321, Smith and Tuttle, 1957; 31-1081, Benedetti et al., 1977). Sufficient differences exist between the X-ray data of synthetic tetrakalsilite (both ours and that of Smith and Tuttle, 1957) and natural panunzite as to make exact equivalence of the two questionable.

Characterization of phases

Figure 1 shows X-ray powder diffraction patterns for various nepheline samples of the synthetic series, including the highly sodic parent material, as well as for tetrakalsilite and kalsilite. Within structure type there is significant shift of peaks to lower 2θ with increasing Ks. The similar patterns of nepheline and tetrakalsilite can be distinguished by analyzing the 2θ region from 30.3 to 31.5° (Cu radiation), where tetrakalsilite has a sequence of four peaks (322, 430, 412, and 520) and nepheline has but one (300). Tetrakalsilite also has a prominent peak (411) at 25.3°, whereas nepheline has none.

Since the most potassic nepheline samples from our work have K contents beyond those for which X-ray data are available, we have recorded in Table 2[1] data for sample 8908 (synthetic series, Ks = 0.629) for diffraction maxima with relative intensities (uncorrected for preferred orientation) of 2 or greater.

Compositional limits of the phases

The nepheline structure was found to exist from the parent material at the sodic end of the natural and synthetic series to mole fractions Ks of 0.57 and 0.63 (and Ks + VAC contents of 0.64 ± 0.01), respectively. Tetrakalsilite was synthesized in both series at Ks of 0.69 ± 0.02 (Ks + VAC content of 0.72 ± 0.02), near the compositions of the materials studied by Smith and Tuttle (1957) and Benedetti et al. (1977). Since all known tetrakalsilite, synthetic and natural, has compositions in this vicinity, it is unlikely that a Ks content of 0.82 is ideal for this mineral as Merlino (1983) suggests. This conclusion is further supported by the synthesis of kalsilite, not tetrakalsilite, at Ks + VAC ≥ 0.80 for both series of the present study. Moreover, since all of these phase transformations are likely to be displacive, the observed room-temperature boundaries may well shift with temperature. There is therefore little certainty that phases observed at room temperature, particularly those near transformation compositions, are equilibrium phases at higher temperature.

A narrow miscibility gap at synthesis temperatures was found to exist between the most potassic nepheline sample and the tetrakalsilite member in each of the two ion-exchange series. This is discussed at greater length by Hovis and Roux (in preparation).

Unit-cell trends: The location of vacancies in nepheline

Unit-cell dimensions and volumes for all series members are reported in Table 3 and in Figures 2–4. Equa-

[1] A copy of Table 2 may be obtained by ordering Document AM-92-487 from the Business Office, Mineralogical Society of America, 1130 Seventeenth Street NW, Suite 330, Washington, DC 20036, U.S.A. Please remit $5.00 in advance for the microfiche.

TABLE 3. Nepheline-kalsilite unit-cell dimensions and volumes

Sample	a (Å)	c (Å)	V (Å^3)
	Natural series		
8311	9.9903(4)	8.3734(5)	723.74(6)
8861	9.9965(5)	8.3821(7)	725.40(7)
8718	10.0092(4)	8.3902(6)	727.95(6)
8811	10.0413(4)	8.4075(6)	734.13(7)
8862	10.0756(5)	8.4262(6)	740.80(7)
8808	10.1012(10)	8.4393(14)	745.72(15)
8925	10.1330(15)	8.4589(22)	752.17(23)
8929	10.1969(9)	8.4868(18)	764.20(15)
8937	10.2013(9)	8.4909(18)	765.24(15)
8928	20.4889(26)	8.5419(17)	3105.40(84)
8807	5.1410(9)	8.6081(20)	197.03(6)
8723	5.1457(4)	8.6353(9)	198.01(3)
8719	5.1589(4)	8.6953(10)	200.41(3)
8860	5.1607(5)	8.7004(12)	200.67(4)
	Synthetic series		
880408	9.9655(5)	8.3561(8)	718.67(8)
8824	9.9792(7)	8.3647(13)	721.38(11)
8825	9.9905(6)	8.3751(8)	723.92(9)
8826	9.9993(5)	8.3849(6)	726.05(7)
8827	10.0412(5)	8.4105(7)	734.38(8)
8834	10.0918(5)	8.4386(9)	744.29(8)
8853	10.1322(9)	8.4578(10)	751.96(13)
8847	10.1753(4)	8.4791(7)	760.28(6)
8908	10.2080(11)	8.4962(23)	766.71(18)
8843	20.4575(25)	8.5326(17)	3092.56(80)
8828	5.1379(5)	8.6087(13)	196.81(4)
8829	5.1511(5)	8.6612(10)	199.03(3)
8823	5.1611(4)	8.7125(10)	200.98(3)

Note: Bracketed quantities are uncertainties in the last decimal places.

tions for least-squares regression lines in these figures are given in Table 4. Note that symmetry constraints require the a dimension of nepheline to be twice that of kalsilite and half that of tetrakalsilite.

The most interesting aspect of the variation of the a dimension with composition occurs within the nepheline structural region of the natural and synthetic series. In both cases a clear break in slope takes place at relatively

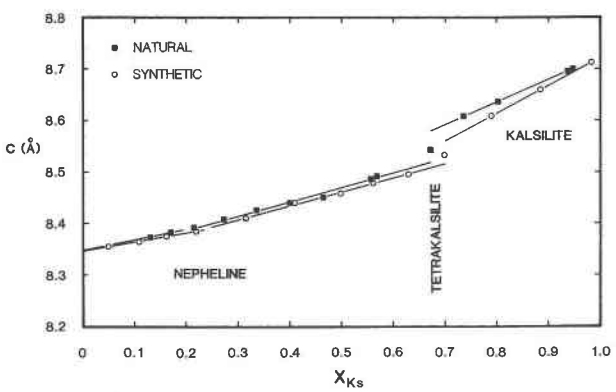

Fig. 3. Variation of the c unit-cell dimension with X_{Ks} (= mole fraction kalsilite). Upper and lower sets of lines are based on least-squares regressions to the natural and synthetic series data, respectively, within each structural region. Because of the presence of vacancies, the most potassic data point for each series is its end point; thus, lines are not extended to the $X_{Ks} = 1$ border. Note the apparent discontinuity in c in the vicinity of $X_{Ks} = 0.7$. Equations for the lines are given in Table 4.

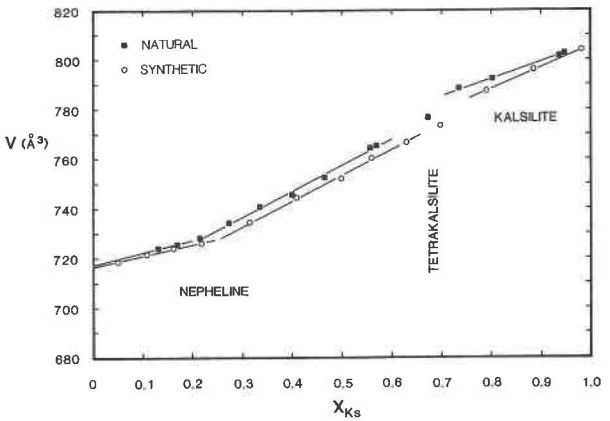

Fig. 4. Variation of unit-cell volume with X_{Ks} (= mole fraction kalsilite). Data for all phases are normalized to the unit cell of nepheline. Upper and lower sets of lines are based on least-squares regressions to the natural and synthetic series data, respectively, within each structural region. Because of the presence of vacancies, the most potassic data point for each series is its end point; thus, lines are not extended to the $X_{Ks} = 1$ border. Equations for the lines are given in Table 4.

sodic compositions (previously recognized by both Smith and Tuttle, 1957, and Donnay et al., 1959), presumably corresponding to the point at which K ions begin to occupy the smaller Na positions of the nepheline structure. Linear least-squares fits for each series based on the variation of a (independently) with Ks, Ne, and 0.5An (the latter for the natural series only) for data near the break ($0.05 < Ks < 0.54$) identified the compositions where the changes in slope occurred, for the natural series at molar K/Na/Ca/VAC = 0.184/0.701/0.032/0.084 and for the synthetic series at 0.238/0.745/0.000/0.017. Considering in both cases that molar Na + Ca is 0.74 ± 0.01 and remembering that the large : small alkali site ratio in nepheline is 0.25:0.75, one might conclude that only Na and Ca occupy the smaller alkali positions for compositions at which the breaks in slope occur. This would in turn imply that a significant number (if not all) of the vacancies in the nepheline structure occupy the larger alkali position. One would reason, then, that in the more silicic vacancy-rich natural series K ions enter the smaller alkali sites at lower molar K content specifically because of the increased fraction of vacancies in that structure and the preference of those vacancies for the larger alkali position.

It is also possible that the change in the slope of a within the nepheline structural region is caused in part by the entry of vacancies into the smaller alkali positions. In this scenario, the tetrahedral framework responds to the □Si substitution by forming a greater proportion of "regular" hexagonal rings (relative to the smaller oval rings), consistent with the wider bond angle of SiOSi vs. SiOAl (Gibbs, 1982) and also with a more symmetric charge distribution in the alkali site, similar to occupancy of the site by a relatively large ion such as K^{1+}. With an

TABLE 4. Coefficients to lines for unit-cell dimensions and volumes shown in Figures 2, 3, and 4

	a_0	a_1	c_0	c_1	V_0	V_1
			Mole fraction (Ks + VAC) = 0.05 to 0.25			
Natural	9.961(7)	0.220(41)	8.348(1)	0.195(7)	717.3(9)	49.0(5.3)
Synthetic	9.956(2)	0.202(13)	8.347(1)	0.173(6)	716.6(2)	44.2(1.5)
			Mole fraction (Ks + VAC) = 0.25 to 0.65			
Natural	9.892(8)	0.538(18)	8.330(2)	0.280(6)	705.3(1.4)	104.3(3.2)
Synthetic	9.873(9)	0.533(17)	8.326(5)	0.271(9)	701.8(1.7)	103.1(3.4)
			Mole fraction (Ks + VAC) = 0.80 to 1.0			
Natural	10.143(8)*	0.187(9)*	8.286(5)	0.437(5)	737.1(2.0)	69.0(2.0)
Synthetic	10.087(18)*	0.240(20)*	8.184(5)	0.538(5)	719.2(3.1)	86.4(3.5)

Note: Equations have the form $q = q_0 + q_1X_{Ks}$, where X_{Ks} is mole fraction kalsilite. Units for a and c are Å; unit for unit-cell volume is Å³.
* Refers to doubled unit cell for kalsilite.

increase in the proportion of regular hexagonal rings, a would increase in much the same manner as if K had replaced Na in the small alkali site. If this mechanism actually operates, the proportion of large : small tetrahedral rings within potassic nepheline would deviate from the ideal 0.25:0.75.

Unit-cell trends: Phase transitions

Since only one tetrakalsilite sample was produced for each series, we do not know the breadth of the compositional range over which this phase occurs. Coupled with the absence of samples in the miscibility gap between potassic nepheline and tetrakalsilite, it is impossible to determine from present data whether discontinuities exist in a at the transitions from nepheline to tetrakalsilite and from tetrakalsilite to kalsilite. From the data in Figure 2, however, it is clear that any such discontinuities would be very small, particularly for the nepheline to tetrakalsilite transition.

The c unit-cell dimension (Fig. 3), however, although displaying the same break in slope as a within the nepheline compositional range, appears to be discontinuous at the transitions from nepheline to tetrakalsilite to kalsilite, evidenced by the intermediate position of the tetrakalsilite data point between projected trends for nepheline and kalsilite. Although it is possible that tetrakalsilite occupies a narrow compositional range, which would "connect" c values of potassic nepheline samples to those of sodic kalsilite samples, there is clearly a discontinuity in c associated with a hypothetical nepheline to kalsilite transition.

Composition parameters

It is impossible to determine unambiguously the composition of a four-component feldspathoid from a single parameter. However, by recognizing that mole fractions

$$K + Na + Ca + VAC = 1 \quad (1)$$

or correspondingly that components

$$Ks + Ne + (\tfrac{1}{2}\cdot 0.5An) + (\tfrac{1}{2}\cdot 0.5An + 2Qz) = 1 \quad (2)$$

one can divide compositional variation into molar (Na + Ca) vs. (K + VAC) and thereby treat this system as a pseudobinary. This would seem to be appropriate in a structural sense, since Na and Ca ions apparently prefer the smaller alkali positions, whereas K ions and vacancies prefer the larger ones. We can also take advantage in the present case of having data for two series that contain different numbers of vacancies. Using the variation of the a unit-cell dimension with combined data for the natural and synthetic series, therefore, we have developed by least-squares regression the following relationships for determination of mole fraction Ks (molar K) in the sodic nepheline, potassic nepheline, and kalsilite structural regions, respectively:

For a between 9.96 and 10.01 Å
$(0.05 < K + VAC < 0.25)$

$$Ks = -47.326\ (\pm\ 2.982) + 4.7547\ (\pm\ 0.2988)\ a - 0.500\ (\pm\ 0.116)\ VAC, \quad (3)$$

for a between 10.01 and 10.21 Å
$(0.25 < K + VAC < 0.65)$

$$Ks = -17.974\ (\pm\ 0.450) + 1.8232\ (\pm\ 0.0444)\ a - 0.709\ (\pm\ 0.100)\ VAC, \quad (4)$$

for a between 10.28 and 10.32 Å
$(0.80 < K + VAC < 1.00)$

$$Ks = -46.543\ (\pm\ 3.034) + 4.6068\ (\pm\ 0.2945)\ a - 1.173\ (\pm\ 0.265)\ VAC, \quad (5)$$

where VAC is mole fraction vacancies. These equations reproduced input data to within 0.016 Ks for all samples and to within 0.011 for all but four of the 25 data points on which they were based. If the VAC term is ignored, application of these equations to vacancy-bearing samples will lead to Ks values that are too potassic.

The X-ray peak that is 201 of nepheline, 401 of tetrakalsilite, or 101 of kalsilite is also useful for composition determination because of its high intensity, continuity over all structures, and sensitivity to K substitution, changing by nearly 1° 2θ from one end-member to the other. Regression equations based on this peak (Cu radiation) for the same three structural regions are as follows:

For 2θ between 23.17 and 23.08°
$(0.05 < K + VAC < 0.25)$

$$Ks = 47.155\ (\pm\ 4.436) - 2.0332\ (\pm\ 0.1918)\ 2\theta_{201} - 0.425\ (\pm\ 0.170)\ VAC, \quad (6)$$

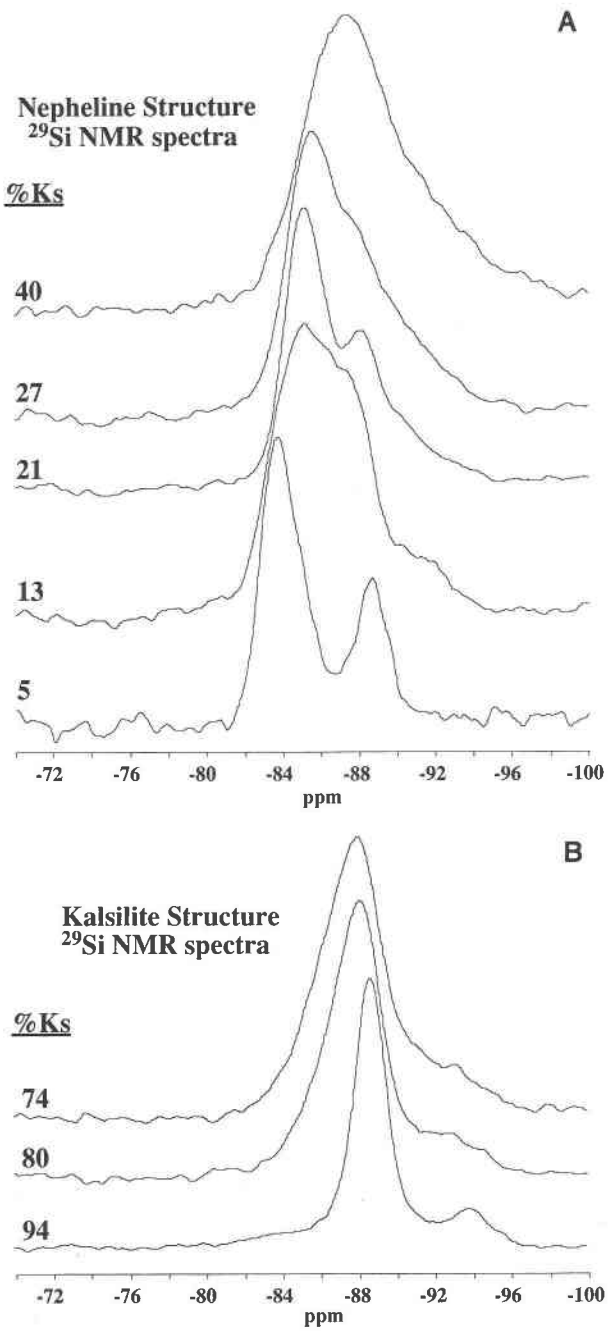

Fig. 5. Diagram of ^{29}Si spectra, arranged by composition, for samples with the nepheline (**A**) and kalsilite (**B**) structure. Note that the Si:Al ratio is different between the Ks_5 and Ks_{13} samples, since the Ks_5 sample is from the synthetic series, whereas all others are from the natural series.

for 2θ between 23.08 and 22.54°
($0.25 < K + VAC < 0.65$)

$$Ks = 20.233\ (\pm\ 0.387) - 0.8655\ (\pm\ 0.0170)\ 2\theta_{201} - 0.680\ (\pm\ 0.081)\ VAC, \quad (7)$$

for 2θ between 22.46 and 22.32°
($0.80 < K + VAC < 1.00$)

$$Ks = 34.862\ (\pm\ 1.604) - 1.5170\ (\pm\ 0.0717)\ 2\theta_{101} - 0.872\ (\pm\ 0.197)\ VAC. \quad (8)$$

These equations reproduced input data as well as those based on a. Given a choice, however, the use of a is preferred, since it is based on data for multiple peaks.

Volumes

It is noteworthy that volumes (Fig. 4) of the natural series are generally greater, at any particular K content, than those of the synthetic series. Counter to one's intuition that the substitution of a vacancy for Na should decrease volume, the overall effect of the coupled □Si = NaAl substitution is to increase volume, evidence that the main effect is tetrahedral. This seems to correlate with the preference of vacancies for the larger alkali positions in nepheline.

Since tetrakalsilite volume data are aligned with the trend for potassic nepheline, there is apparently little or no volume change associated with the nepheline to tetrakalsilite transition. However, either a tetrakalsilite to kalsilite or a hypothetical nepheline to kalsilite transition at $K + VAC = 0.72$ would be accompanied by a positive volume change of about 7 Å^3 (or 0.013 cal/bar·mol), based on the nepheline unit cell. This discontinuity affects interpretation of the volumes of K-Na mixing for these series (Hovis and Roux, in preparation).

NMR RESULTS

NMR techniques

All NMR experiments were conducted at room temperature on a Varian VXR-400 spectrometer (9.395 T field) using a Varian MAS probe at spinning speeds of 3–5 kHz with zirconia rotors. Chemical shifts for the ^{29}Si, ^{27}Al, and ^{23}Na spectra were measured relative to tetramethylsilane (TMS), *1M* aqueous $Al(NO_3)_3$, and *1M* aqueous NaCl, respectively. The following samples from the natural series were used for the NMR part of this study: 8311, 8718, 8811, and 8808, all having the nepheline structure, and 8807, 8723, and 8719 with the kalsilite structure. In addition, 880408 (Ks = 0.050) was used from the synthetic series.

Spectra observations for ^{29}Si

In a previous study of natural and synthetic phases in the nepheline-kalsilite system, Stebbins et al. (1986) showed that Al avoidance is maintained, resulting in nearly complete Si-Al order. This contrasted with long-range disorder reported in some previous X-ray studies (Hahn and Buerger, 1955; Dollase, 1970; Foreman and Peacor, 1970). The two crystallographically unique sites in the nepheline structure (a general site, T_G, with two Na and one K neighbor, and a special site, T_S, with three Na neighbors) produced the two major peaks in the ^{29}Si MAS spectra, with area ratios of approximately 3:1. The kalsilite structure, with all T sites equivalent, produced a single major peak. Minor peaks at more negative chemical shifts were attributed to extra sites resulting from

excess Si. Our new results for Monte Somma nepheline and kalsilite (Figs. 5A and 5B) are very similar to those of this previous study.

The 3:1 ratio of the two sites is also clearly seen in our new data for the Ks_5 nepheline. At increasing Ks contents, the peaks broaden and the T_G (left-most) peak moves to lower frequency (more negative chemical shift). For the most K-rich nepheline studied (8808, Ks_{40}), the two peaks have broadened and merged. The contrast between the Ks_5 and Ks_{13} samples is enhanced by additional broadening in the latter (and more Ks-rich samples) as a result of the additional disorder from the presence of $Ca_{0.5}AlSiO_4$ and SiO_2 components. The line shape of the latter sample appears also to be somewhat anomalous, possibly because it was not annealed at 800 °C during ion exchange.

Samples having the kalsilite structure (Fig. 5B) have single major ^{29}Si MAS peaks. Again, there is extra intensity at lower frequency attributable to Si sites with three instead of four Al neighbors, resulting from excess Si. As for the nepheline structures, compositional changes away from stoichiometry (increasing Ne content) result in broader NMR peaks. These shift systematically to higher frequency, approaching those for the most Ks-rich nepheline.

Spectra observations for ^{27}Al

The ^{27}Al spectra follow a trend broadly similar to that of the ^{29}Si spectra (Figs. 6A and 6B). The Ks_5 sample has two distinct peaks with approximately 3:1 area ratios representing the T_G and T_S Al sites. Note that there is no intensity to the high frequency side of these peaks as would be expected if there were any Al-O-Al linkages, thus preserving the Al avoidance rule. These peaks broaden and move closer together, and the center of gravity of the peaks shifts to lower frequency as Ks increases within the nepheline structure. Again, the peaks for the Ks_5 sample are best resolved, probably because of the lack of disorder caused by the nonbinary compositions of the other samples. The ^{27}Al spectra for the kalsilite samples also show a trend similar to that for the ^{29}Si spectra, broadening and shifting to higher frequency as the nepheline component in the kalsilite increases. The line shape of the spinning sidebands in the ^{27}Al spectra follow similar changes as the central transitions with composition.

Spectra observations for ^{23}Na

The ^{23}Na spectra for samples with the nepheline structure show a slight broadening and shift with composition, similar to the Al and Si spectra although not as pronounced (Figs. 7A and 7B). This is most likely due to the much broader initial line widths of the Na spectra, which cause any additional broadening to be less discernible. For K + VAC > 0.25 only one Na peak is present, which is consistent with a high degree of ordering between K and Na atoms between the two types of alkali sites, with Na preferentially located in the smaller of the two sites (Hahn and Buerger, 1955; Dollase, 1970; Gregorkiewitz, 1984). For samples with K + VAC < 0.25 two Na NMR peaks are evident, since Na occupies two different alkali sites in this composition region. The excess Na in the K site is evident as a small shoulder on the right side of the Ks_{13} spectra. For samples with the kalsilite structure, the ^{23}Na line broadens as the composition becomes more sodic, but there is little shift in position.

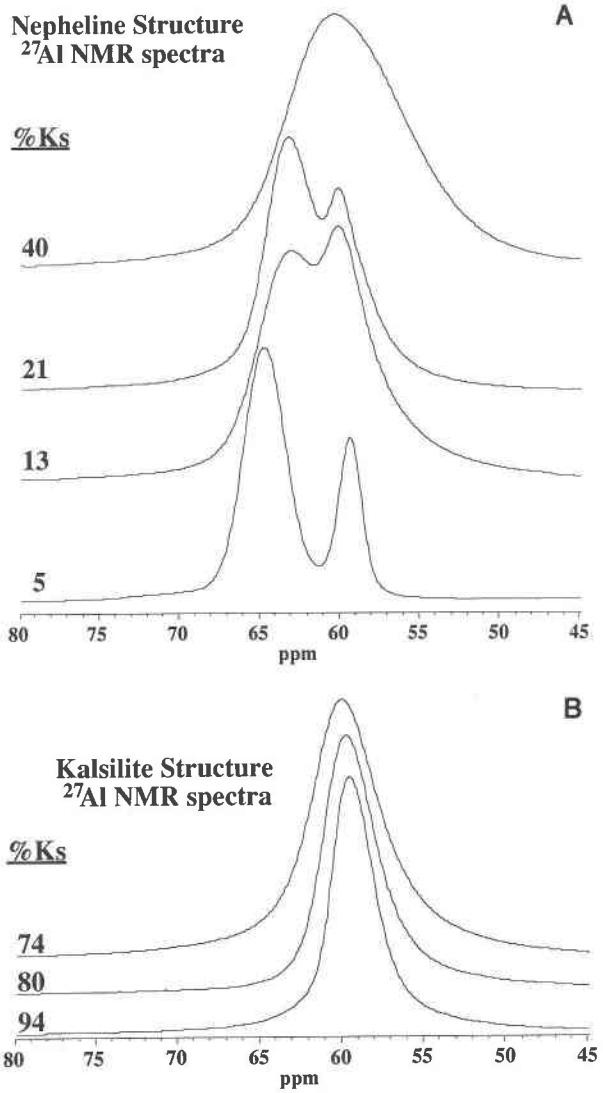

Fig. 6. Diagram of ^{27}Al spectra for samples with the nepheline (**A**) and kalsilite (**B**) structure, from the natural series except for Ks_5.

Thus, we observe the same overall trend with composition for all of the nuclei studied. With an increase in Ks in the nepheline samples, a broadening of the lines is observed along with a shift of the center of gravity toward lower frequency. An increase in the sodic component in the kalsilite structure has the same effect but in the opposite direction; that is, the lines broaden, but the center of gravity moves toward higher frequency. Qualitatively,

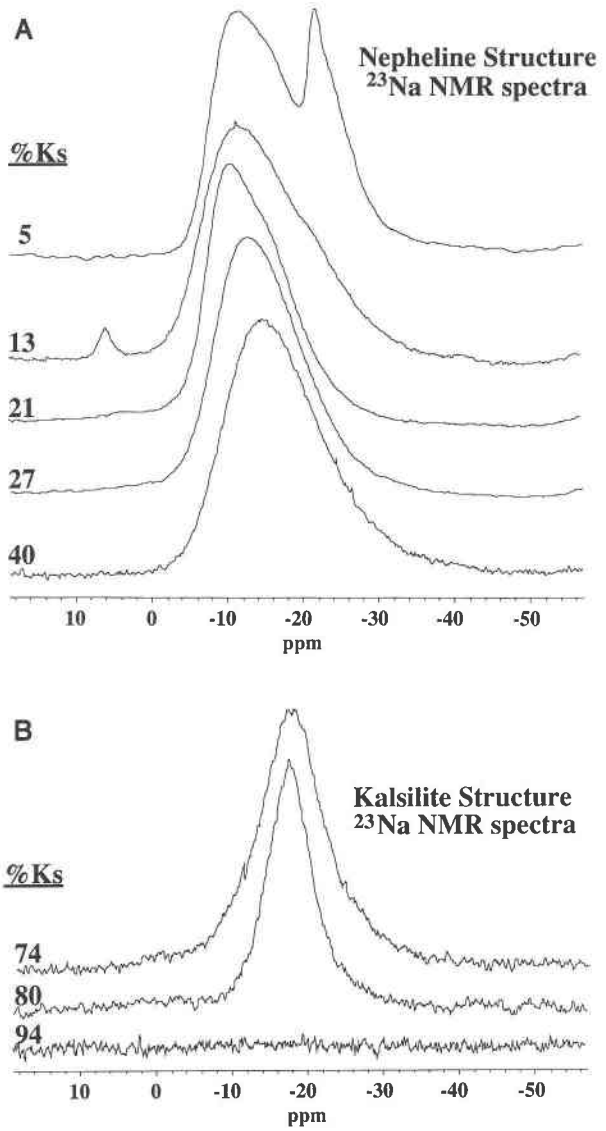

Fig. 7. Diagram of ^{23}Na spectra for samples with the nepheline (**A**) and kalsilite (**B**) structure, from the natural series except for Ks_5. The small peak near 5 ppm on the 13% Ks spectrum is probably caused by a small amount of an unknown impurity. The latter had no detectable effect on calorimetric results (Hovis and Roux, in preparation).

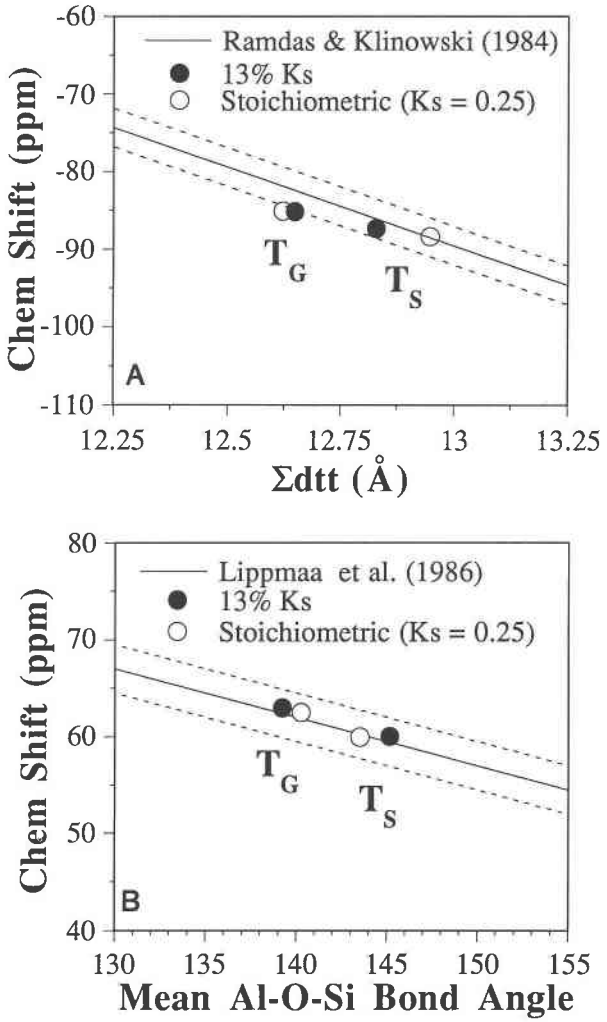

Fig. 8. Plots of chemical shift vs. mean Si-Al bond distance (**A**) for ^{29}Si and mean Al-O-Si bond angle (**B**) for ^{27}Al. Dashed lines indicate approximate scatter of original data from which the lines were regressed. T_G = general site: tetrahedral site surrounded by 2 Na and 1 K. T_S = special site, with site symmetry of 3, surrounded by 3 Na atoms.

this can be interpreted as a distortion of the structures toward one another as their compositions grow closer.

Calculations

Chemical shift has been shown to be correlated with the mean Si-Al intratetrahedral distance in the case of ^{29}Si NMR (Ramdas and Klinowski, 1984) and with the mean Al-O-Si bond angle in the case of ^{27}Al NMR (Lippmaa et al., 1986). Chemical shift data from the nepheline samples in this study have therefore been combined with mean Si-Al bond distances calculated for the two unique Si sites and with mean Al-O-Si bond angles for the two unique Al sites in the nepheline structure based on X-ray data from several sources (Dollase, 1970; Foreman and Peacor, 1970; Gregorkiewitz, 1984). The structural data calculated from Gregorkiewitz (1984) and Dollase (1970) were averaged to approximate the structure of the 13% Ks (8311) sample and plotted against the chemical shift data from this sample. The nepheline used by Foreman and Peacor (1970), reported as stoichiometric nepheline from Bancroft, Ontario, was plotted against the chemical shift of a Bancroft plutonic nepheline from Stebbins et al. (1986). The data (Figs. 8A and 8B) are in good agreement with the plots from Lippmaa et al. (1986) and Ramdas and Klinowski (1984) and fall within the scatter of the original data from which these lines were regressed. In addition, the decreasing ^{29}Si and ^{27}Al chem-

Table 5. Mean centers of gravity for the $m = 3/2$ sidebands, central $m = 1/2$ transition, and calculated C_Q

Ks	Average position, T_G (ppm) $m = 3/2$	$m = 1/2$	$\sigma(3/2) - \sigma(1/2)$	C_Q (MHz)*
5	66.21	64.69	1.52	1.56
13	64.22	62.96	1.27	1.43
21	63.64	63.20	0.44	0.85
40	63.10	60.14	2.96	2.18
74	62.30	60.03	2.27	1.91
80	62.12	59.68	2.44	1.98
94	61.77	59.45	2.32	1.93

* C_Q calculated assuming $\eta = 0$.

ical shifts with increasing K content reported in the above section are consistent with an increase in the mean Al-O-Si angle, and the broadening of the ^{29}Si lines away from Ks_{21} suggests an increase in the width of the distribution of the Al-O-Si angles.

In addition to spectral line widths, another measure of the distortion of a crystallographic site is the quadrupolar coupling constant (C_Q), which is the product of the largest component of the electric field gradient (EFG) tensor and the nuclear quadrupolar moment (eQ). The nuclear quadrupolar moment is constant for any given nucleus; therefore C_Q is a function only of the EFG. By calculating C_Q, a relative measurement of the distortion on a given site is obtained. In general, the larger the quadrupolar coupling constant, the more distorted a site is from spherical symmetry (Ghose and Tsang, 1973). For any given nucleus, the relative quadrupolar shift of the center of gravity $\sigma_{QS}(m)$ of a single quantum (m, $m - 1$) transition powder pattern line shape is given by the following expression:

$$\sigma_{QS}(m) = -\frac{3}{40}\frac{C_Q^2}{\omega_L^2}\frac{I(I+1) - 9m(m-1) - 3}{I^2(2I-1)^2}\left(1 + \frac{\eta^2}{3}\right) \quad (9)$$

(Lippmaa et al., 1986) where ω_L = Larmor frequency, I = spin quantum number, m = quantum transition, and η = asymmetry parameter of the EFG ($0 \leq \eta \geq 1$). For a given nucleus, ω_L, m, and I are all known, which leaves finding values for $\sigma_{QS}(m)$ and η to solve for C_Q. However, $\sigma_{QS}(m)$ need not be known directly to solve for C_Q. One can measure the difference in the shift of the centers of gravity of the $m = 1/2$ and $m = 3/2$ transitions [i.e., $\sigma(3/2) - \sigma(1/2)$] by comparing the average position of the low-order $m = 3/2$ spinning sidebands and the position of the central transition (Lippmaa et al., 1986). For a given transition, the observed center of gravity of the peak (σ_{CG}) is shifted from the true isotropic chemical shift (σ_{CS}) by the second-order quadrupolar shift (σ_{QS}):

$$\sigma_{CG}(m) = \sigma_{CS} + \sigma_{QS}(m). \quad (10)$$

Since σ_{CS} is independent of the transition, the difference between the observed centers of gravity for two different transitions will be the same as the difference between their

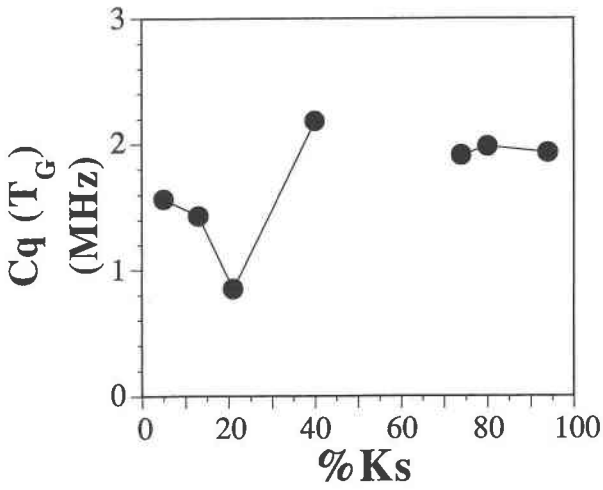

Fig. 9. Plot of quadrupolar coupling constant (C_Q), calculated from ^{27}Al spinning sidebands vs. composition.

quadrupolar shifts. Thus, for ^{27}Al, which had the most clearly resolved sidebands ($I = 5/2$, $m = \pm 1/2$, $\pm 3/2$, or $\pm 5/2$, and $\omega_L = 104.214$ MHz), Equation 9 reduces to

$$\sigma_{QS}(1/2) = -5.5246 \times 10^{-13} C_Q^2\left(1 + \frac{\eta^2}{3}\right) \quad (11)$$

$$\sigma_{QS}(3/2) = 6.9057 \times 10^{-14} C_Q^2\left(1 + \frac{\eta^2}{3}\right) \quad (12)$$

for the $m = \pm 1/2$ and $\pm 3/2$ transitions, respectively, with C_Q in Hz and σ_{QS} in ppm. The difference in the shift of the centers of gravity, and hence the quadrupolar shift, of the $m = 1/2$ and $m = 3/2$ transitions for Al is thus

$$\sigma_{QS}(3/2) - \sigma_{QS}(1/2) = 6.2152 \times 10^{-13} C_Q^2\left(1 + \frac{\eta^2}{3}\right). \quad (13)$$

Therefore, for a given value of η, the quadrupolar interaction constant C_Q can be calculated for each of the spectra and compared to determine relative site distortions. A list of the measured mean centers of gravity for the $m = 3/2$ sidebands, central $m = 1/2$ transition, and calculated C_Q values for the T_G site is given in Table 5. The T_S peak was not resolved well enough in the sidebands to allow for an adequate determination of C_Q for the special site. The $m = 5/2$ sidebands were also not used because they showed poor resolution.

A plot of C_Q vs. composition for the general Al site (T_G) in the nepheline and kalsilite samples is given in Figure 9. This method is not very sensitive to the value of η, and the same general trend is observed on a C_Q vs. composition plot over the range of possible η values. Thus, we have calculated values of C_Q based on the arbitrary assumption that $\eta = 0$. The sample closest to stoichiometric nepheline in composition (8718, Ks_{21}) is observed to have the smallest C_Q, whereas the most potassic nepheline studied (8808, Ks_{40}) has the largest value of C_Q. The

samples on the kalsilite side of the solvus show nearly constant values of C_Q.

Summary

The K exchange of natural and synthetic nepheline during this investigation produced three phases, as observed at room temperature: nepheline, tetrakalsilite, and kalsilite. From the Na end of each series unit-cell dimensions and volumes were found to increase linearly with composition. The abrupt increase in the slopes of these lines for nepheline near K + VAC = 0.25 reflects the entry of K ions into the smaller Na positions of the structure but may also in part result from the entry of vacancies into these positions and the associated formation of a greater proportion of regular hexagonal (Si-rich), tetrahedral rings in the nepheline structure. Changes in these slopes at lower Ks values in the relatively vacancy-rich natural series indeed evidence the preference of vacancies for the larger alkali site of nepheline. This and the fact that the $\square Si = NaAl$ substitution actually causes an increase in volume suggest that it is the increased Si in the framework, and not the occupancy of the alkali site by a hole, that governs the resulting physical behavior of the mineral.

Discontinuities were found to exist in the c unit-cell dimension at the nepheline to tetrakalsilite transition and in both c and volume at the tetrakalsilite to kalsilite phase transition. These observations in turn correlate with only minor enthalpy effects at the nepheline-tetrakalsilite and tetrakalsilite-kalsilite transitions (Hovis and Roux, in preparation).

Changes in unit-cell size and shape reflect the long-range average distortion of the structure. The local nature of these changes with composition is demonstrated by the NMR results. Peak positions for ^{29}Si, ^{23}Na, and ^{27}Al all shift in response to the overall change in structure, and quadrupolar broadening increases as the solvus is approached, indicating that distortion does indeed accompany changes in the average unit-cell shape. However, some of the broadening in the ^{23}Na and ^{27}Al lines and most of the broadening in the ^{29}Si lines must result from an increase in local scale disorder. As K is added to stoichiometric nepheline, or Na to kalsilite, local distortions occur to accommodate the nonideal cation, generating populations of sites with bond angles and distances (and chemical shifts) different from the average. Consequences of this local disorder may be quite significant for both entropy and enthalpy.

The ^{29}Si and ^{27}Al NMR also confirm that the Al avoidance rule is obeyed by these samples and that there is little or no disorder of Al and Si among the tetrahedral sites. The slight excess (5.2%) of Si in the natural series gives rise to excess intensity on the lower frequency side of the Si peaks, which is attributed to a Si with three Al and one Si next nearest neighbors. If there were any significant amount of Al with Al next nearest neighbors, one would expect to see a similar "excess" of intensity in the ^{27}Al spectra, which is not observed. Thus, we conclude that the excess Si in the samples is distributed randomly among the tetrahedral sites and that the Al avoidance rule is preserved.

Finally, the discontinuity of structural response to compositional changes seen in the long-range structure is quite apparent at the local scale. It is clear from the NMR data that, at least with respect to adding K to 0.25 Ks nepheline or Na to 100% kalsilite, the modeling of configurational entropy will need to take into account not only the mixing of cations and vacancies on alkali sites but also the variation in distortion among tetrahedra.

Acknowledgments

We wish to thank Enrico Franco (Naples University) for the nepheline specimen from Monte Somma, and Stefano Merlino (Pisa University), who put us in contact with Franco. Michael Carpenter (University of Cambridge) kindly did TEM work to check two of our samples for homogeneity. We also thank the University of Cambridge for electron microprobe analysis of sample 880408. Jason Kelsey of Lafayette College helped with X-ray analyses in preliminary stages of this project. We thank Brian Phillips and an anonymous reviewer for valuable comments in their reviews of this manuscript. Daniel Rogers kindly helped with proofreading. We gratefully acknowledge financial support for this research from the Earth Sciences Division of the National Science Foundation under grants EAR-8616403 (to G.L.H.) and EAR-8707175 and EAR-8905188 (to J.F.S.).

References cited

Benedetti, E., De Gennaro, M., and Franco, E. (1977) Primo rinvenimento in natura de tetrakalsilite. Rendiconti Accademia Nazionale Dei Lincei Classe Di Scienze Fisiche Matematiche E Naturali, Series VIII, 62, 835–838.

Burnham, C.W. (1962) Lattice constant refinement. Carnegie Institution of Washington Year Book, 61, 132–135.

Dollase, W.A. (1970) Least-squares refinement of the structure of a plutonic nepheline. Zeitschrift für Kristallographie, 132, 27–44.

Donnay, G., Schairer, J.F., and Donnay, J.D.H. (1959) Nepheline solid solutions. Mineralogical Magazine, 32, 93–109.

Foreman, N., and Peacor, D.R. (1970) Refinement of the nepheline structure at several temperatures. Zeitschrift für Kristallographie, 132, 45–70.

Ghose, S., and Tsang, T. (1973) Structural dependence of quadrupole coupling constant e^2qQ/h for ^{27}Al and crystal field parameter D for Fe^{3+} in aluminosilicates. American Mineralogist, 58, 748–755.

Gibbs, G.V. (1982) Molecules as models for bonding in silicates. American Mineralogist, 67, 421–450.

Gregorkiewitz, M. (1984) Crystal structure and Al/Si-ordering of a synthetic nepheline. Bulletin de Minéralogie, 107, 499–507.

Hahn, T., and Buerger, M.J. (1955) The detailed structure of nepheline, $KNa_3Al_4Si_4O_{16}$. Zeitschrift für Kristallographie, 106, 308–338.

Hamilton, D.L., and Henderson, C.M.B. (1968) The preparation of silicate composition by a gelling method. Mineralogical Magazine, 36, 832–838.

Henderson, C.M.B., and Roux, J. (1977) Inversion in subpotassic nephelines. Contributions to Mineralogy and Petrology, 61, 279–298.

Keller, L., and McCarthy, G.J. (1984) JCPDS grant-in-aid report (International Center for Diffraction Data file no. 35-424).

Lippmaa, E., Samoson, A., and Mägi, M. (1986) High-resolution ^{27}Al NMR of aluminosilicates. Journal of the American Chemical Society, 108, 1730–1735.

Merlino, S. (1983) Feldspathoids: Their average and real structures. In W.L. Brown, Ed., Feldspars and feldspathoids: Structures, properties and occurrences, p. 435–470. Reidel, Dordrecht, The Netherlands.

Ramdas, S., and Klinowski, J. (1984) A simple correlation between isotropic ^{29}Si-NMR chemical shifts and T-O-T angles in zeolite frameworks. Nature, 308, 521–523.

Smith, J.V., and Tuttle, O.F. (1957) The nepheline-kalsilite system: I. X-ray data for the crystalline phases. American Journal of Science, 255, 282–305.

Stebbins, J.F., Murdoch, J.B., Carmichael, I.S.E., and Pines, A. (1986) Defects and short-range order in nepheline group minerals: A silicon-29 nuclear magnetic resonance study. Physics and Chemistry of Minerals, 13, 371–381.

Manuscript received October 4, 1990
Manuscript accepted September 16, 1991